Bull. Chem. Soc. Jpn., 71, 1581—1585 (1998)

Nascent Internal-State Distribution of Product OH($A^2\Sigma$) Observed in a Crossed Beam Reaction of Hot H Atom with N_2O

Shinji Tsuboi, Toshihiro Sawai, Hiroshi Ohoyama,* and Toshio Kasai*

Department of Chemistry, Graduate School of Science, Osaka University, Toyonaka, Osaka 560-0043

(Received January 30, 1998)

The chemiluminescence spectrum of product OH($A^2\Sigma$) in a crossed beam reaction of the hot H atom with N_2O was observed for the first time. The nascent internal-state distribution of OH($A^2\Sigma$) was identified by spectral simulation. The rotational distribution was found to be characterized by a Boltzmann temperature of 750±100 K, and the vibrational distribution is non-Boltzmann with the populations of $v=0$, 1, and 2 being 1 : 0.75 : 0.15, respectively. These results indicate that the product rotation is poorly excited while vibration is highly excited to the contrary.

Since it is known that the reaction of the H atom with N_2O is important in flame chemistry and in atmospheric chemistry, especially in NO_X pollution, it has been extensively studied to clarify the reaction mechanisms from experimental and theoretical points of view.[1,2] So far, the following reaction channels are reported for the H+N_2O bimolecular reaction.[3—7]

$$H+N_2O \rightarrow OH(X^2\Pi)+N_2(X^1\Sigma) \quad \Delta H=-62.8 \text{ kcal mol}^{-1} \quad (1)$$

$$\rightarrow OH(A^2\Sigma)+N_2(X^1\Sigma) \quad \Delta H=30.6 \text{ kcal mol}^{-1} \quad (2)$$

$$\rightarrow NH(X^3\Sigma)+NO(X^2\Pi) \quad \Delta H=30.2 \text{ kcal mol}^{-1} \quad (3)$$

Hollingsworth and co-workers have investigated reaction 1 using the hot H atoms generated by 248-nm laser photolysis of HI, and they studied the rotational distribution of OH($X^2\Pi$) by the LIF technique.[8] Wittig and co-workers have made comparative experiments of the H+N_2O bimolecular reaction under bulk conditions and also the intra-cluster reaction of HX·N_2O (X = Br, I) under precursor geometry-limited conditions.[3,9—16] For chemiluminescent reaction 2, only one study has been done on the OH($A^2\Sigma$) formation from the 193-nm photolysis of the HBr/N_2O gas mixture by Wittig and co-workers.[9,10] They have measured the OH($A^2\Sigma$) chemiluminescence spectrum and estimated the nascent vibrational distribution of $v=0$, 1, and 2 as 1 : 0.6 : 0.4 without spectral simulation. They conclude that the OH($A^2\Sigma$) formation is feasible only for the bimolecular reaction and not for the HBr·N_2O intra-cluster reaction.[9,10,12]

Such bulk conditions, however, may not be the best for studying gas-phase reactions because of unavoidable side reactions. The 193-nm photolysis of the HX/N_2O gas mixture for reaction 2, for instance, could produce O(^1D) from N_2O in addition to the hot H atoms from HX. Therefore it is likely that the O(^1D)+HX reaction would additionally take place and produce OH($A^2\Sigma$).[17] Another possibility one may think of is that the hot H atoms initially produced may be deenergized by collisions in the reaction cell when the radiative lifetime of product is long. For these reasons, it is indispensable to study these elementary reactions by use of crossed beams, although the weak signal intensity always makes experiment difficult. We use crossed beams of the H atom and a free jet N_2O for the first time in order to clarify the elementary bimolecular reactions of H+N_2O→OH($A^2\Sigma$)+N_2. The OH($A^2\Sigma$) chemiluminescence indeed is observed, thus the comparison can be made between the obtained internal-state distribution of OH($A^2\Sigma$) and the previous bulk results in the 193 nm photolysis of the HBr/N_2O gas mixture.

Experimental

A schematic drawing of the experimental setup is shown in Fig. 1. The apparatus consists of a source chamber for the hot H-atom beam, and a reaction chamber. These are differentially pumped down to $<1\times10^{-6}$ Torr (1 Torr = 133.322 Pa), respectively. The operating pressure with the beams was kept less than 5×10^{-5} Torr all the time. The N_2O pulsed valve (1 mmϕ i.d.) is operated at 150 Torr and 30 mm behind the cross beam region in the reaction chamber. A pulsed HBr beam with 500-μs duration emerges from a pulsed valve (0.8 mmϕ i.d.) at the stagnation pressure of 100 Torr. The hot H atoms are produced in the source chamber by 193 nm light of a ArF excimer laser (50—100 mJ) which is focused into a 2×5 mm area that is 3 mm from the HBr pulsed valve. The distance between the irradiation point and the cross beam point is 40 mm. In order to reduce stray lights from the laser radiation, a series of light baffles are used. The H atoms are collimated by a 5-mmϕ beam collimator. Since the photodissociation of HBr at 193 nm produces both Br($^2P_{3/2}$) and Br($^2P_{1/2}$) atoms, the hot H atoms with the different velocities 2.26×10^6 and 2.06×10^6 cm s^{-1} can be prepared, respectively.[18,19] To eliminate charged species in the H-atom beam after laser irradiation, a pair of deflecting plates (100 V cm^{-1}) are placed before the beam collimator. For the radiative lifetime measurement, the total chemiluminescence from the cross beam region is collected by a concave mirror and focused onto a photomultiplier (Hamamatsu R1635P). The time evolution of the emission is recorded by a multichannel scaler (Stanford Research

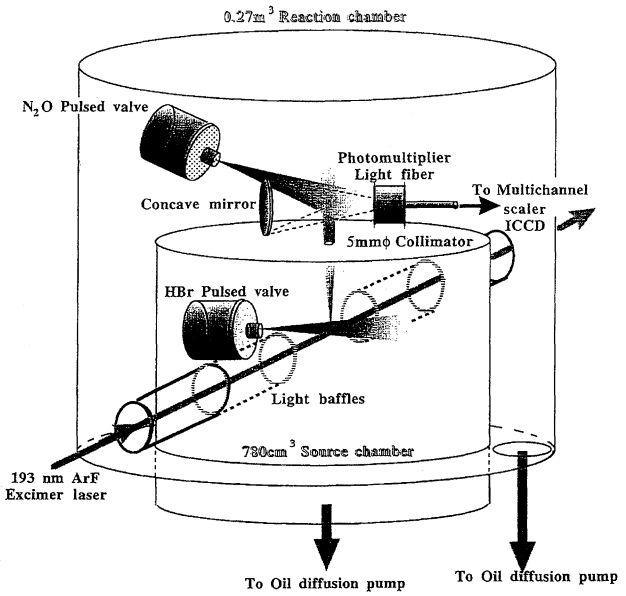

Fig. 1. Schematic drawing of the experimental arrangement.

Systems SR430) with the gate width of 5 ns.

For the measurement of the chemiluminescence spectrum, the light emission is focused into one end of a light fiber which ends up with a monochromator entrance followed by a gated intensified CCD detector (ICCD; ORIEL 77193-5). The ICCD detector records emission spectra over the wavelength range from 275 to 327 nm. The gate width of the ICCD is set as 3 μs and delayed for 1.5 μs after laser irradiation. All trigger pulses are generated by a delay-pulse generator (Stanford Research Systems DG535) controlled by a micro computer. The optical calibration of the monochromator and the ICCD detector is done by the atomic lines of a low-pressure Hg lamp. The wavelength resolution of 2.5 nm and the slit function are measured for the spectral simulation use. The sensitivity curve of the detection system on wavelength was determined using a standard Br lamp (Ushio JPD500WCS).

Results and Discussion

a. Assignment of the Emitter in H+N_2O Reaction. Figure 2 shows the time evolution of the chemiluminescence after the 193 nm laser irradiation. The time origin was set to the laser irradiation for the hot H-atom generation. The emission signal gave an instant rise after 1.8 μs and this delay time was found to be in good agreement with the flight time of the hot H atoms from the beam source, and the decay rate of the chemiluminescence signal gave an excellent coincidence with the radiative lifetimes of ca. 700 ns for OH($A^2\Sigma$), (either $\tau_0(v=0)=693\pm30$ ns for $v=0$, or $\tau_1(v=1)=736\pm33$ ns for $v=1$).[20,21] The time profile of Fig. 2 thus suggests that the light emission is responsible for the product OH($A^2\Sigma$) from the reaction of the hot H atom with N_2O.

The dependence of the emission intensity on the stagnation pressure of N_2O is plotted in Fig. 3. The chemiluminescence intensity was found to be proportional to the N_2O pressure, indicating that the emission product is produced by single collision with respect to the N_2O reactant. At 150 Torr of the N_2O stagnation pressure, the formation of $(N_2O)_n$ clusters is expected to be negligible.[22]

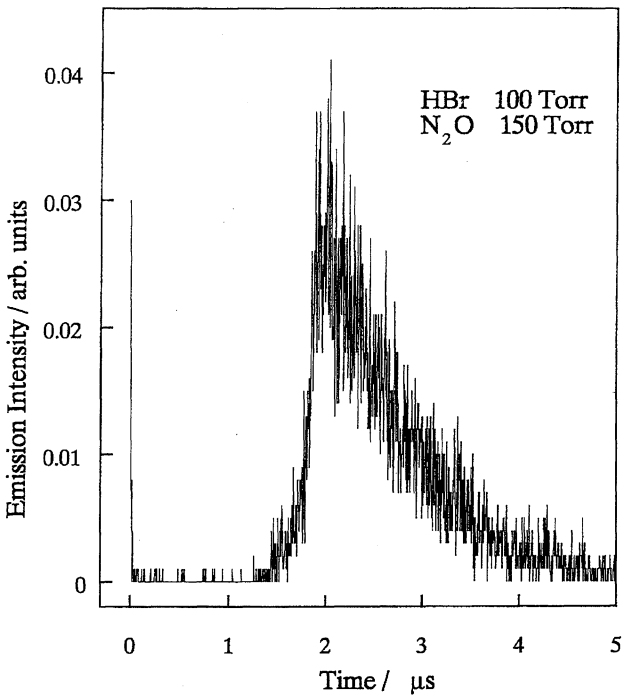

Fig. 2. Time evolution of the OH(A–X) chemiluminescence measured with 5 ns gate width. The origin in time is the time of excimer laser irradiation.

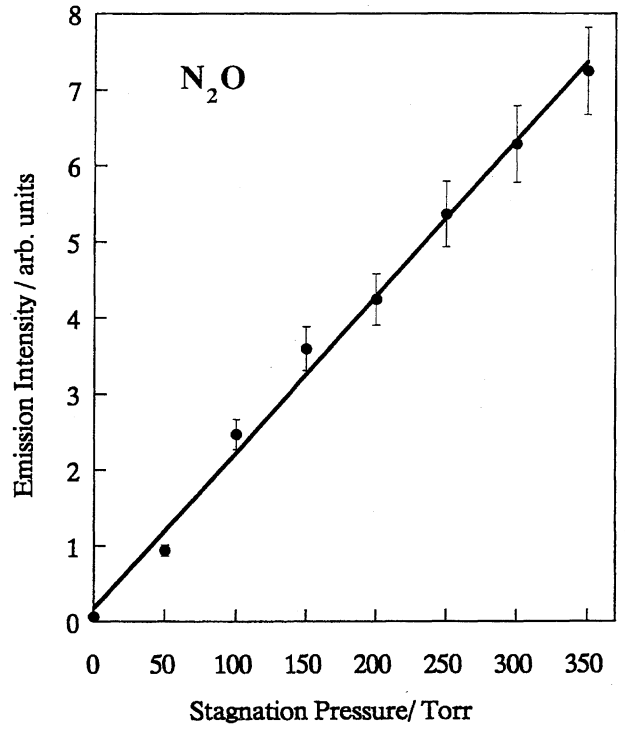

Fig. 3. Chemiluminescence intensity is plotted vs the stagnation pressure of N_2O. The stagnation pressure of HBr is set at 100 Torr.

In order to confirm that the emitter is OH($A^2\Sigma$), the emission spectrum was measured. According to the time profile of Fig. 2, the sampling gate of ICCD was set as 3 μs and 1.5 μs delay. The observed spectrum is shown in Fig. 4A. The

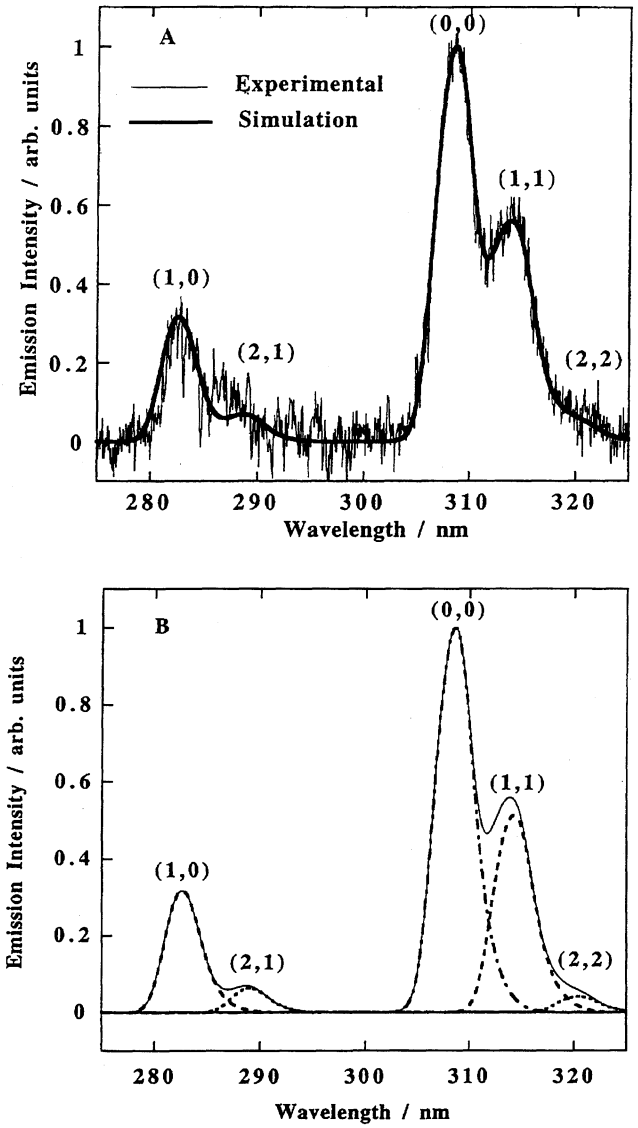

Fig. 4. A: (—) Experimental chemiluminescence spectrum of OH($A^2\Sigma$), with the resolution of 2.5 nm FWHM. (—) Simulated spectrum. B: Simulated spectrum. As a reference, the contributions from each vibrational band were shown.

peaks centered at 282, 308, and 314 nm could be assigned as the (1,0), (0,0), and (1,1) vibrational bands of the OH(A–X) transition, respectively as shown in the figure.[23—27] The chemiluminescent reaction (2) indeed occurs and the product is assigned as OH($A^2\Sigma$).

b. Initial-State Distribution of OH($A^2\Sigma$). The spectral simulation was done to identify the initial-state distribution of OH($A^2\Sigma$). The spectral resolution was found to be unsatisfactory for resolving each rotational line because of the weak crossed-beam signal, the rotational distribution was assumed to be a Boltzmann distribution $P_v(N')$ for each vibrational state. There are twelve branches in the rotational transition and the relative line strengths for each rotational line were calculated based on the Hönl–London factors $S_b(N')$ (cited from Ref. 23), and the Franck–Condon factors $q_{v'v''}$ (cited from Ref. 24). As described in the previous section, the experimentally measured slit function $\rho(\lambda)$ was used as the spectral line shape in this simulation. The spectral resolution was set as equal to the experimental value of 2.5 nm. The vibrational state populations were obtained as the best-fit parameters of the simulation. Predissociation of OH($A^2\Sigma$) is reported to take place for the rotational states above $N'=23$ for $v=0$, and above $N'=14$ for $v'=1$, also for all those states of $v'=2$.[28] In order to estimate the contribution due to such predissociation in the spectral simulation, the rotational states in the sum were extended over $N'_{v=0}=23$, $N'_{v=1}=14$, and $N'_{v=2}=10$. The total intensity I in each wavelength was calculated by the following equation.

$$I=\sum_{N=1}^{N}\sum_{v'=0}^{2}\sum_{b=1}^{12} q_{v'v''}\nu^3\frac{S_b(N')}{2N'+1}P(v')P_v(N')\rho(\lambda) \qquad (4)$$

$$(N: N'_{v=0}=23,\ N'_{v=1}=14,\ N'_{v=2}=10)$$

The best-fit result of the simulation is shown in Fig. 4A. Since the vibrational band-envelope was found to be sensitive to the rotational distribution $P_v(N')$, the rotational temperature of each vibrational state had to be estimated independently. However, the rotational temperature turned out to be the same as 750±100 K. As a reference, Fig. 4B shows a deconvoluted spectrum of simulated vibrational bands in the spectrum. In spite of the poor spectral resolution, overlap of the vibrational bands have little influence on the peak height of each vibrational band at each of the peak positions. Therefore, the vibrational populations can be measured rather precisely within the limit of the experimental *S/N* ratio. Thus, the vibrational populations for $v=0$, 1, and 2 are found to be 1 : 0.75 : 0.15, respectively. Since all rotational states of $v=2$ are known to have a strong character of predissociation with a lifetime of 270±25 ns,[20,21] the population for $v=2$ must be corrected to 1.0. The rotational and vibrational distributions obtained by this simulation are summarized in Table 1. The fractional energies released in rotation and vibration are calculated to be $\langle f_r\rangle=0.048$, $\langle f_v\rangle=0.21$ where we assume that the available energy for reaction 2 is 30.9 kcal mol^{-1}, which clearly shows strong excitation in vibration.

c. Spectral Comparison to the Bulk Experiment. So far, only one study has been done for the OH($A^2\Sigma$) formation from the 193-nm photolysis of the HBr/N_2O gas

Table 1. The Vibrational Distribution and Rotational Boltzmann Temperatures of Nascent OH($A^2\Sigma$)

	$v=0$	$v=1$	$v=2$
Vibrational distribution	1.0	0.75±0.05	0.15±0.05 (1.0±0.3)[a]
	1.0*	0.6*	0.4*
Rotational temperature (K)	750	750	750

a) The value in the parenthes was estimated by taking into account the short lifetime for all states of $v=2$ due to the predissociation.
b) *The distribution reported by Wittig et al.

mixture. They have measured the $OH(A^2\Sigma)$ chemiluminescence spectrum and estimated the nascent vibrational distribution of $v = 0$, 1, and 2 as 1 : 0.6 : 0.4 without spectral simulation.[9,10] In order to understand the difference from their result and to check the effects from Franck–Condon factors, tow additional simulations were done by using the different Franck–Condon factors cited from Ref. 23, which was used in the previous report by Wittig et al., Simulation 1 is for these results and simulation 2 is based on the vibrational distribution by Wittig and co-workers. These are shown in Fig. 5. It was confirmed that the difference of the Franck–Condon factors between Refs. 23 and 24 has little effect on the simulated result, and that this result obtained under the crossed beam conditions is significantly different from the previous one. There is a possibility that the $OH(A^2\Sigma)$ produced from the 193 nm photolysis of the HBr/N_2O gas mixture has some contribution from the reaction of $O(^1D)+HBr \rightarrow OH(A^2\Sigma, v = 0)+Br$. In addition, the simulation showed that the spectrum reported by Wittig et al. has some discrepancies. For example, the relative intensity of the (1, 1) band with respect to that of the (1, 0) band seems to be nearly unity, although it must be about 2 from the Franck–Condon factor requirement (see the relative intensity for the (1, 1) band with the (1, 0) band in Fig. 4B).

The potential energy surface for the $H+N_2O \rightarrow OH(A^2\Sigma)+N_2$ reaction is not well known because its reactant surface cannot be correlated directly to the product surface. Thus, the crossing of the two surfaces must be important in reaction 2. At the initial stage of this reaction, however, one would expect the direct and also the indirect mechanisms just like in reaction 1, i.e. $H+N_2O \rightarrow OH(X^2\Pi)+N_2(X^1\Sigma)$. Wittig et al. have reported that $OH(A^2\Sigma)$ formation has a threshold between 2.5 and 1.82 eV.[10] Therefore, it is estimated that the highly excited state of HON_2 would correlate to the $OH(A^2\Sigma)$ formation. This process may correspond to the direct mechanism. On the contrary, since $OH(A^2\Sigma)$ is efficiently quenched by N_2 via a strongly-attractive interaction,[29] there is at least one adiabatic surface correlating to $OH(A^2\Sigma)+N_2(X^1\Sigma)$ that does not have a barrier associated with the final separation of the $OH(A^2\Sigma)$ and $N_2(X'\Sigma)$ fragments. This process may be attributed to the indirect mechanism. In the indirect mechanism, the 1,3 migration of the H atom in the $[HNNO]^*$ intermediate should occur after the formation of the O–H bond. This mechanism would make the rotational distribution highly excited as compared with the direct mechanism. On the other hand, the direct mechanism would give a high vibrational excitation of $OH(A^2\Sigma)$, and in turn a poor rotational excitation of $OH(A^2\Sigma)$. Recently, Schatz and coworkers have reported that the direct mechanism is the main channel in the bimolecular reaction 1. One could therefore expect that the formation of $OH(A^2\Sigma)$ would also proceed via the direct mechanism, which may be consequently favorable at the O-end of N_2O. If this is the case, a large orientation dependence is expected for reaction 2. This question is a future issue that may be solved using an oriented N_2O beam.[30]

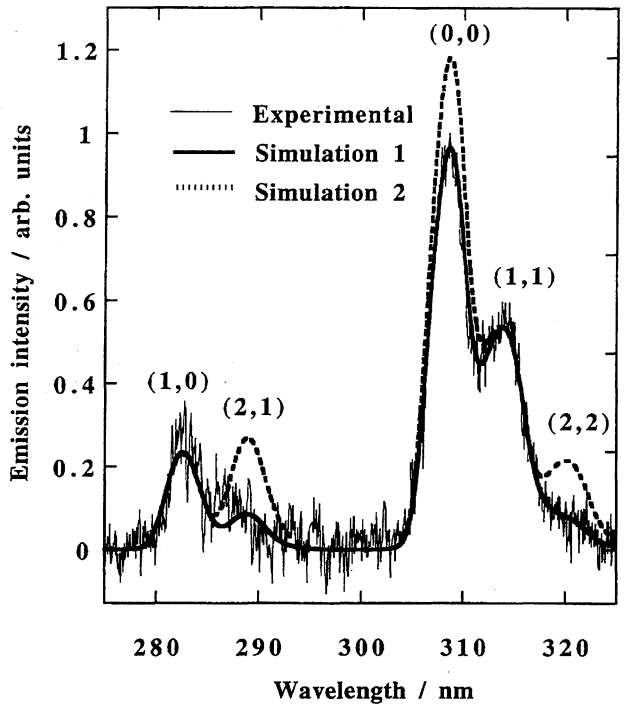

Fig. 5. Comparison of the vibrational distribution with the result by Wittig et al.. (—) Experimental chemiluminescence spectrum of $OH(A^2\Sigma)$ in the crossed beam condition. (present result). (—) Simulation 1: Simulated spectrum for the present result by using the Franck–Condon factors in Ref. 23. (····) Simulation 2: Simulated spectrum based on the vibrational distribution by Wittig et al. by using the Franck–Condon factors in Ref. 23.

This work was supported by a Grant-in-Aid on Priority-Area-Research "Photoreaction Dynamics" No. 06239239 from the Ministry of Education, Science and Culture. We thank Mitsubishi Foundation for financial support in purchasing the ICCD detection system.

References

1) R. J. Cattolica, M. D. Smooke, and A. M. Dean, *Sandia Rep. SAND82*, **1982**, 8776.

2) W. R. Andersen, L. J. Decker, and A. J. Kotlar, *Combust. Flame*, **48**, 179 (1980).

3) G. Dixon-Lewis and D. J. Williams, in "Gas-Phase Combusion, Comprehensive Chemical Kinetics," ed by C. H. Bamford and C. F. H. Tipper, Elsevier, Amsterdam (1977), Vol. 17.

4) P. Marsall, A. Fontijin, and C. F. Melius, *J. Chem. Phys.*, **86**, 5540 (1987).

5) K. S. Bradley and G. C. Schatz, *J. Chem. Phys.*, **100**, 12154 (1996).

6) S. P. Walch, *J. Chem. Phys.*, **98**, 1170 (1993).

7) K. S. Bradley, P. McCabe, G. C. Schatz, and S. P. Walch, *J. Chem. Phys.*, **102**, 6696 (1995).

8) W. E. Hollingsworth, J. Subbiah, G. W. Flynn, and R. E. Weston, Jr., *J. Chem. Phys.*, **82**, 2295 (1985).

9) G. Hoffmann, D. Oh, H. Iams, and C. Wittig, *Chem. Phys. Lett.*, **155**, 356 (1989).

10) G. Hoffmann, D. Oh, and C. Wittig, *J. Chem. Soc., Faraday Trans. 2*, **1989**, 85 and 1141.

11) G. Hoffmann, D. Oh, Y. Chen, Y. Engel, and C. Wittig, *Isr.*

J. Chem., **30**, 115 (1990).
12) S. K. Shin, Y. Chen, E. Böhmer, and C. Wittig, "Regioselective Photochemistry in Weakly Bonded Complexes," ed by M. Stuke, Topics in Applied Physics, Springer Verlag, Berlin (1992), Vol. 70, p. 57.
13) H. Ohoyama, M. Takayanagi, T. Nishiya, and I. Hanazaki, *Chem. Phys. Lett.*, **162**, 1 (1989).
14) Y. P. Zeng, S. W. Sharpe, D. Reifschneider, C. Wittig, and R. A. Beaudet, *J. Chem. Phys.*, **93**, 183 (1990).
15) S. K. Shin, C. Wittig, and W. A. Goddard, III, *J. Phys. Chem.*, **95**, 8048 (1991).
16) E. Böhmer, S. K. Shin, Y. Chen, and C. Wittig, *J. Chem. Phys.*, **97**, 2536 (1992).
17) H. Okabe, "Photochemistry of Small Molecules," Wiley, New York (1978).
18) F. Magnotta, D. Nesbitt, and S. R. Leone, *Chem. Phys. Lett.*, **83**, 21 (1981).
19) Z. Xu, B. Kopltz, and C. Wittig, *J. Phys. Chem.*, **92**, 5518 (1988).
20) K. R. German, *J. Chem. Phys.*, **62**, 2584 (1975).
21) K. R. German, *J. Chem. Phys.*, **63**, 5252 (1975).
22) K. Honma, Y. Fujimura, and O. Kajimoto, *J. Chem. Phys.*, **88**, 4739 (1988).
23) H. M. Crosswhite and G. H. Dieke, *J. Quant. Spectrosc. Radiat. Transfer*, **2**, 97 (1962).
24) L. Klein, *J. Quant. Spectrosc. Radiat. Transfer*, **13**, 581 (1973).
25) D. R. Crosley and R. K. Lengel, *J. Quant. Spectrosc. Radiat. Transfer*, **15**, 579 (1975).
26) W. L. Dimpfl and J. L. Kinsey, *J. Quant. Spectrosc. Radiat. Transfer*, **21**, 233 (1979).
27) I. L. Chidsey and D. R. Crosley, *J. Quant. Spectrosc. Radiat. Transfer*, **23**, 187 (1980).
28) R. A. Sutherland and R. A. Anderson, *J. Chem. Phys.*, **58**, 1226 (1973).
29) D. R. Clrosly, *J. Phys. Chem.*, **93**, 6273 (1989).
30) H. Ohoyama, S. Tsuboi, and T. Kasai, *Chem. Lett.*, **16**, 947 (1995).